

# Studies on the Photo-Oxidation of PP and PP/mLLDPE Blend Systems: Thermal, Physicochemical, and Mechanical Behavior

A. P. Gupta,<sup>1</sup> U. K. Saroop,<sup>2</sup> Vidya Gupta<sup>1</sup>

<sup>1</sup>Department of Applied Chemistry and Polymer Technology, Delhi College of Engineering, University of Delhi, Delhi 110042, India

<sup>2</sup>Reliance Industries Limited, Swastik Mill Compound, V. N. Purav Marg, Chembur, Mumbai 400071, India

Received 19 January 2007; accepted 12 March 2007

DOI 10.1002/app.26762

Published online 3 July 2007 in Wiley InterScience (www.interscience.wiley.com).

**ABSTRACT:** The photo-oxidative degradation of the blends of polypropylene (PP) with metallocene linear low density polyethylene (mLLDPE) were studied. The blend samples were exposed to the ultraviolet radiation (UV) for a period of 6 weeks. Tensile mechanical characteristics were derived from stress–strain curves. The changes in crystallinity during exposure were followed by X-ray diffraction (XRD) and differential scanning calorimetry (DSC), whereas the chemical degradation of the blend samples was evaluated by FTIR-ATR. In case of PP, tremendous decrease is observed in tensile strength, elongation at break, and

increase is observed in tensile modulus with exposure time. However, with the addition of mLLDPE, UV stability of PP has significantly improved. A significant increase in crystallinity during UV exposure was noted for PP, whereas for PP/mLLDPE (80/20) blend system the crystallinity did not change much. Therefore low level of stabilizers may be required for PP/mLLDPE blend systems. © 2007 Wiley Periodicals, Inc. *J Appl Polym Sci* 106: 917–925, 2007

**Key words:** polypropylene; mLLDPE; photo-degradation; DSC; XRD; FTIR

## INTRODUCTION

Polypropylene (PP) is a thermoplastic with a number of desirable properties that make it a versatile material. However, poor impact properties especially at low temperature, poor stability towards ultraviolet (UV) light limit some of its applications. To achieve better properties impact modifiers have been added to PP.

Blending of different plastic resins has long been practiced to tailor make blends for specific processing and performance requirements. About 30% of total annual production of polymers is used in blends, and about 80% of these blends are manufactured to improve toughness of the matrix polymer. Toughness of polymeric material is the decisive parameter used in material selection for a wide variety of applications. In outdoor applications, all polymers degrade no matter how strong or tough the materials may be. Many of those parts, having been exposed to UV light for long periods of time are heavily photo-oxidized because of the relative high photo-sensitivity, especially if they were made of PP; hence changes are expected in the thermal behavior,

mechanical properties, and surface morphology of the products.<sup>1–5</sup>

Photo-degradation of LDPE/PP blend,<sup>6</sup> PC/PP blend,<sup>7</sup> blends of PP with recycled PP<sup>8</sup> has been studied. PP/LDPE blends compatibilized with rubber-PP-graft copolymers or ethylene-propylene-diene-monomer rubber (EPDM) copolymer have been reported more susceptible to be photo-oxidized than incompatible blends.<sup>9</sup> The blending of LDPE and iPP has been reported to increase the oxidative stability of PP.<sup>10</sup> Blends of PP with rubber such as butyl rubber, polyisoprene, polybutadiene, and styrene-butadiene-rubber (SBR) decrease the oxidative stability of PP.<sup>11</sup> UV stability of PP decreased by blending with LDPE, ethylene-vinylacetate copolymer (EVA), EPDM, or their combinations.<sup>12</sup>

A number of studies have been devoted to the degradation and stabilization of conventional polymers; however, very few studies have been found to the use of metallocene polymers and their blend systems.<sup>13–19</sup> As metallocene catalyzed mLLDPE has a low degree of unsaturation and a low level of metal residue, it should exhibit a high intrinsic oxidative stability.<sup>16</sup>

In present article, mechanical, thermal, and physico-chemical properties of PP/mLLDPE blends with the variation of mLLDPE content from 10 to 20% before and after photo-oxidative degradation have been described. The aim of present work is to

Correspondence to: A. P. Gupta (dr\_ap\_gupta@yahoo.co.in or drapgupta@gmail.com).

observe changes in crystallinity caused by photo-oxidation and the extent of chemical degradation by FTIR-ATR. The mechanical properties were also investigated.

## EXPERIMENTAL

### Materials

1. PP Repol H110MA from Reliance Industries Ltd., Hazaria (Gujarat) India, MFI-(230°C/2.16 kg)—11.0 g/10 min.
2. mLLDPE (Engage-8150) of Dow Chemicals (USA), which contains 15% octene as a comonomer with ethylene. MFI-(190°C/2.16 kg)—0.5 g/10 min.

### Preparation of blends

Blends of PP with mLLDPE at levels ranging from 10 to 20% were prepared by melt compounding on a Berstoff ZE-25 twin screw extruder ( $L/D = 40:1$ ) equipped with corotating screws. The granules of PP and mLLDPE were dry mixed in appropriate ratios. The mixture was then fed into the hopper of the extruder. The blending was carried out at screw speed of 200 rpm and a temperature profile of 200-230-240-235-225°C from first zone to the die. The screw speed was adjusted to attain a constant torque level of 90 Nm in all cases. The strands obtained from the extruder were cut into small granules in a granulator. Designation and percent composition of various blend systems are given in Table I.

The blends were then converted into standard ASTM test specimens by injection molding on Windsor SP180 machine and tested for mechanical properties. During injection molding, shot size of  $\sim 350$  g, clamping force of 180 tons, and screw speed of 56 rpm were adjusted.

### Exposure conditions

The tensile bars and impact test pieces were subjected to QUV (Q-Panel UVB-313 tubes) lamp chamber for UV aging. The total intensity used was about  $0.65 \text{ W/m}^2$  in the wavelength region 290–320 nm. Their output matches closed with solar radiation in the ultraviolet range of the spectrum. The QUV

lamp chamber was operated according to the ASTM D-4329-99 method, selecting 8 h UV irradiation at  $(60 \pm 1)^\circ\text{C}$  and 4 h condensation at  $(50 \pm 1)^\circ\text{C}$  cycle continuously.<sup>20</sup> After the required aging time, the samples were taken out of the QUV lamp chamber for characterization. Impact test samples were used for FTIR-ATR, X-ray diffraction (XRD), and differential scanning calorimetry (DSC) analysis.

### Measurements

#### X-ray diffraction analysis

The XRD pattern was recorded at room temperature with a Philips Analytical X-ray diffractometer (PW3710). The radiation from the Cu target was reflected from a graphite monochromator to obtain monochromatic  $\text{Cu K}\alpha$  radiation with a wavelength of 0.1541 nm. The generator was operated at 40 kV and 20 mA. The diffractograms were determined over a range of diffraction angle  $2\theta$  from  $10^\circ$  to  $40^\circ$  with a step size of  $0.02^\circ$ .

XRD is a primary technique to determine the degree of crystallinity in polymers. From the relationship of the peak area to the total area, crystallinity can be evaluated.

$$\% \text{ Crystallinity} = \frac{I_{\text{cr}}}{I_{\text{cr}} + I_{\text{am}}} \quad (1)$$

where  $I_{\text{cr}}$  is an integral intensity of the crystalline phase and  $I_{\text{am}}$  is integral intensity of the amorphous phase.

The apparent dimensions of a crystallite  $L_{hkl}$  along the direction perpendicular to the crystal plane  $hkl$  can be determined using the Scherrer equation

$$L_{hkl} = \frac{K\lambda}{\beta_0 \cos \theta} \quad (2)$$

where  $L_{hkl}$  is the crystalline size along the direction perpendicular to reflection plane ( $hkl$ ) in nanometers,  $\theta$  is the Bragg angle,  $\lambda$  is the wavelength of X-ray used (0.1541 nm),  $\beta_0$  is the peak width of diffraction beam used (rad),  $K$  is the shape factor of crystalline, being related to the shape of a crystalline and definition of  $\beta_0$ , when  $\beta_0$  is defined as the half-height width of diffraction peak,  $K = 0.9$ .

The relative content of  $\beta$ -form in PP were determined using the Turner-Jones equation<sup>21</sup> on the basis of a typical XRD diagram,

$$k = \frac{H_{\beta 1}}{H_{\beta 1} + (H_{\alpha 1} + H_{\alpha 2} + H_{\alpha 3})} \quad (3)$$

where  $k$  is the amount of  $\beta$  form,  $H_{\beta 1}$  is the height of the strong single  $\beta$  form (300), and  $H_{\alpha}$  is the three equatorial  $\alpha$ -form peaks (110), (040), (130).

TABLE I  
Compositional Details of Blends of Polypropylene  
with mLLDPE

Blend code	Polypropylene (wt %)	mLLDPE (wt %)
PP/mLLDPE	100	0
PP/mLLDPE (90/10)	90	10
PP/mLLDPE (80/20)	80	20

**TABLE II**  
Crystalline Size and  $\beta$ -Form Crystal Content of Photo Degraded PP and Their Blends

Blend code	Exposure time (weeks)	$L_{110}$ (Å)	$L_{040}$ (Å)	$L_{130}$ (Å)	$\beta$ -form crystal content (%)
PP (100/0)	0	3.880	3.504	3.90	16.86
	1	4.366	3.890	5.85	14.30
	2	4.980	3.890	7.00	13.52
	3	5.720	4.852	7.02	12.8
	6	6.980	14.018	7.02	6.2
PP/mLLDPE (90/10)	0	4.360	3.504	3.512	16.96
	1	3.490	3.890	4.380	14.02
	2	3.490	4.370	5.850	12.98
	3	6.980	7.280	2.926	9.4
	6	8.732	14.01	8.782	6.1
PP/mLLDPE (80/20)	0	3.880	7.788	8.78	14.81
	1	4.365	8.760	7.02	11.25
	2	6.980	10.01	7.02	9.59
	3	8.730	10.04	8.78	8.33
	6	11.64	23.66	11.64	4.1

#### Differential scanning calorimetry

The crystallization and melting behavior of the blend samples were studied by DSC using a Perkin-Elmer DSC-7 in a nitrogen atmosphere in the heating and cooling rate of 20°C/min. In the first heating and cooling scans, the samples were heated from 50 to 220°C, held at that temperature for 1 min to eliminate thermal history, and then the nonisothermal crystallization process was recorded from 220 to 50°C, and a standard status of crystallization was created. Second heating was done at the same scanning rate as the first heating, whereby the melting characteristics of the samples were recorded. The crystallinity  $X_c$  was calculated by relative ratio of the enthalpy of fusion per gram of samples ( $\Delta H_f^{\text{obs}}$ ) to the heat of fusion ( $\Delta H_f^0$ ) of PP crystal (209 J/g).<sup>22</sup>

$$\% \text{ Crystallinity } X_c = \left( \Delta H_f^{\text{obs}} / \Delta H_f^0 \right) \times 100 \quad (4)$$

#### Fourier transform infrared-attenuated total reflectance analysis (FTIR-ATR)

FTIR-ATR analysis was carried out for degraded samples to measure the extent of chemical degradation. Infrared spectra were obtained in transmission with a Perkin Elmer FTIR-ATR. The equipment was set to operate in the range 600–4000  $\text{cm}^{-1}$ . A carbonyl index was computed as the relative areas under the carbonyl peak (1700–1800  $\text{cm}^{-1}$ ) and a reference peak, not affected by photo-oxidation (centered at 2720  $\text{cm}^{-1}$ ).

#### Tensile properties

The tensile properties were measured using a Lloyd universal tester (model LR10K plus) at  $(23 \pm 2)^\circ\text{C}$  with dumbbell shape specimens at a crosshead speed

of 50 mm/min and with an initial gauge length of 50 mm. Tensile modulus ( $E$ ) and elongation at break ( $E_b$ ) was recorded.

## RESULTS AND DISCUSSION

### Crystallization behavior

Structural parameters of the crystalline regions obtained by the X-ray diffractograms are summarized in Table II. In Figure 1 the X-ray diffractograms of PP photo-degraded for different times are compared. As can be seen in Figure 1 ultraviolet radiation did not cause any substantial change in the position of the peaks. The significant change was observed in the height of the amorphous background, which got reduced with exposure, reflecting the increase in crystallinity. Both XRD and DSC provide measurements of change in crystallinity during UV exposure. Figures 2 and 3 shows that percent

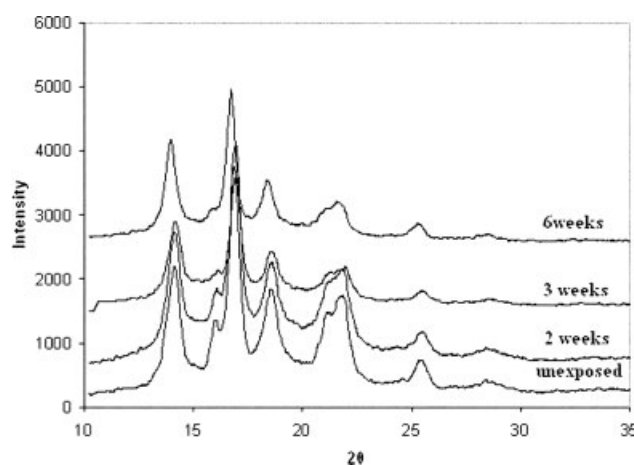


**Figure 1** XRD diffractograms of PP exposed for different times.

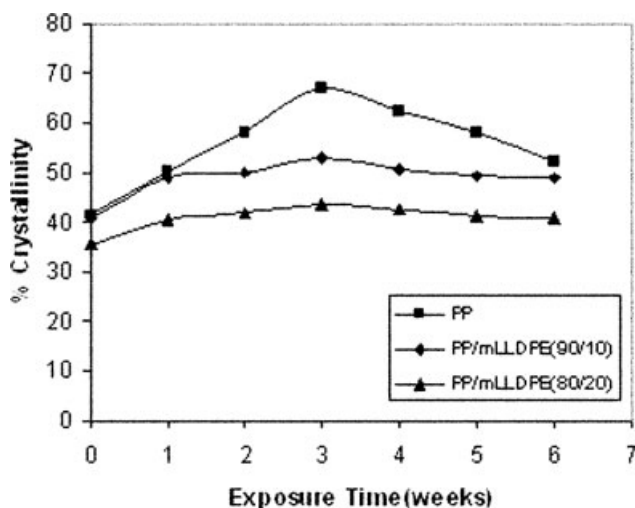


**Figure 2** Percentage crystallinity as a function of exposure time, by XRD.

crystallinity (%X) of PP and PP/mLLDPE blend systems increases with UV exposure time.<sup>3</sup> It is observed that with the progress in photo-oxidation, the number of chain scission events increased and so did the degree of crystallinity. This process is called chemi-crystallization.<sup>3</sup> The highest values of percent crystallinity (%X) are observed for the PP and the smallest ones for PP/mLLDPE blend systems. This indicates that the blending of PP and mLLDPE increases the oxidative stability of PP, presumably because of the dilution of tertiary alkyl radicals of the PP by the domains of mLLDPE, which is in agreement with Waldman and DePaoli.<sup>10</sup>

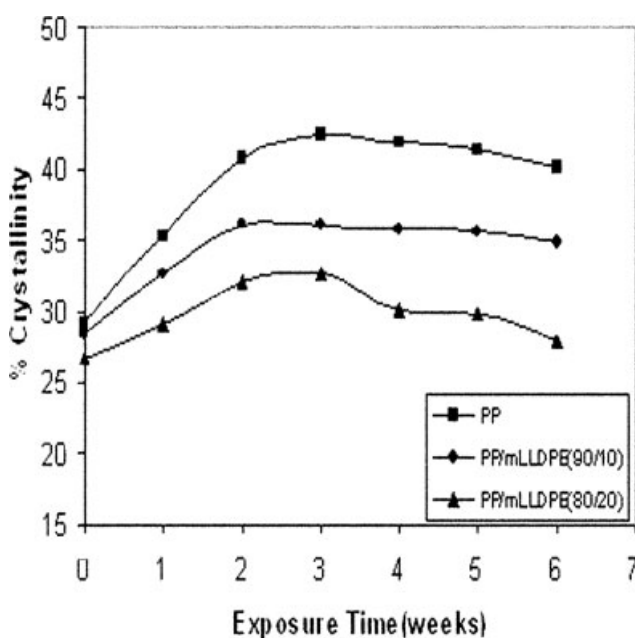
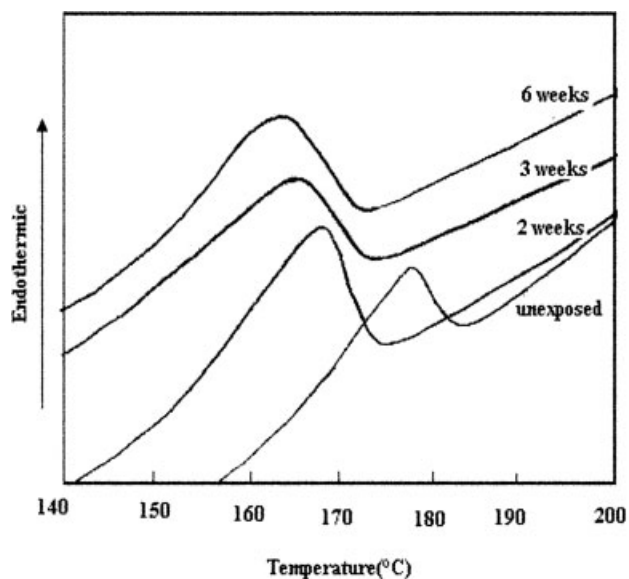
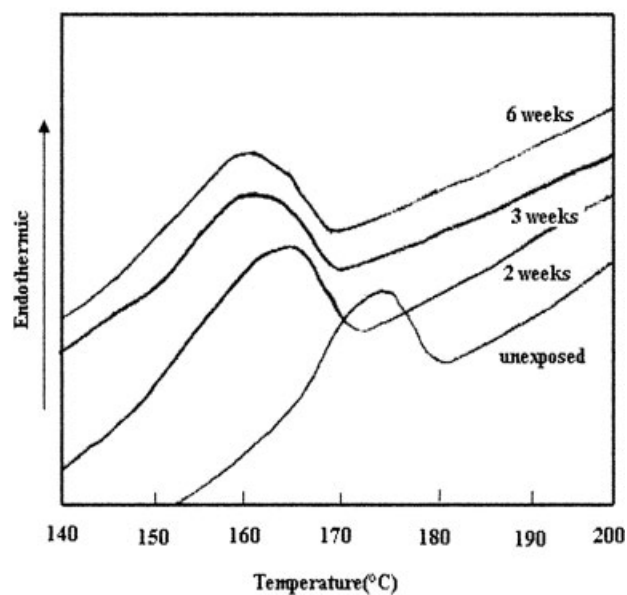


**Figure 3** Percentage crystallinity as a function of exposure time, by DSC.

The important peaks characteristic of the  $\alpha$  phase can be found at the scattering angle  $2\theta$  of  $14.0^\circ$  (110),  $17.0^\circ$  (040),  $18.5^\circ$  (130),  $21.0^\circ$  (111), and  $22.0^\circ$  (131 and 041), whereas the  $\beta$  phase can be detected by peak at  $16^\circ$  (300). It can also be seen that for injection molded PP and their blend samples there is some  $\beta$ -form, which is usually found in PP samples that have been subjected to mechanical deformation, for example, in injection molded and extruded products. The relative content of  $\beta$ -form and crystalline size are listed in Table II. It can be seen from Table II that the  $\beta$ -form



(a)



(b)

**Figure 4** DSC thermogram for PP after selected exposure time (a) first heating run, (b) second heating run.

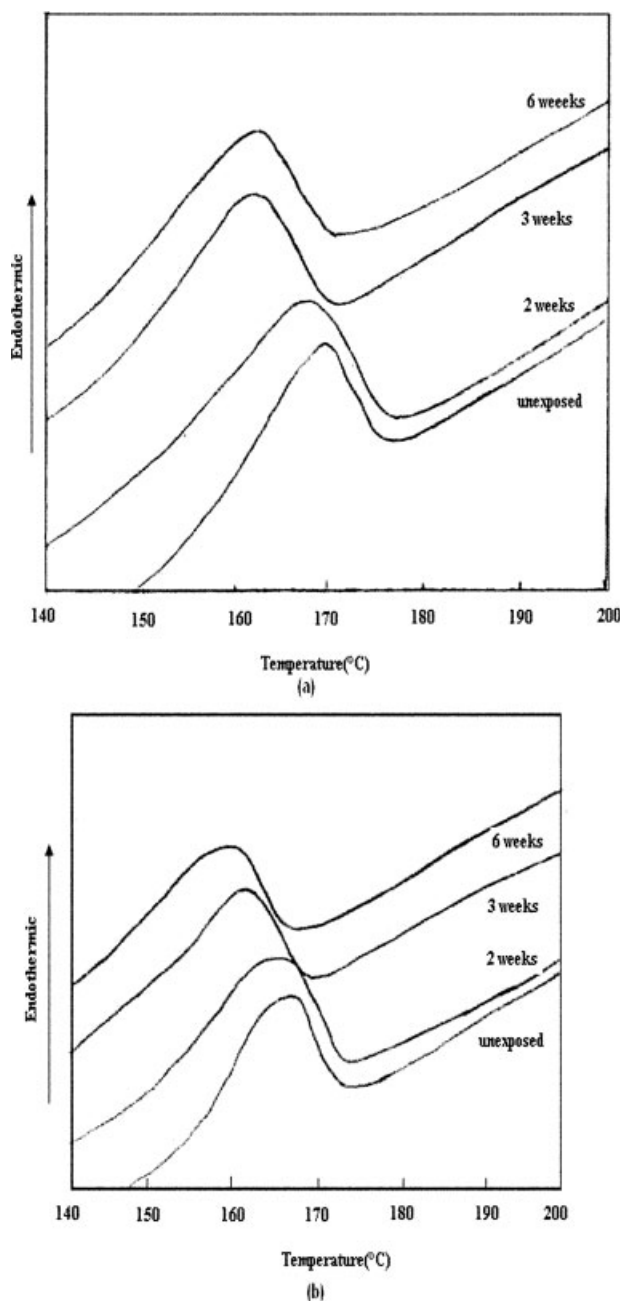


**Figure 5** DSC thermogram for PP/mLLDPE (90/10) after selected exposure time (a) first heating run, (b) second heating run.

content decreases with increasing UV exposure indicating that UV exposure induces the transformation of crystalline form, namely  $\beta$ -form changing into  $\alpha$ -form. The transformation of the less stable  $\beta$ -form into the  $\alpha$ -form upon heating or annealing has been since long known.<sup>23</sup> Its possible explanation is that the molecular chains, which compose  $\beta$ -form relatively lose compared with  $\alpha$ -form and are prone to be photo-degraded to shorter molecular chains, which rearrange into relative stable  $\alpha$ -form. It is also interesting to note that the crystalline size increases with increasing

UV exposure, which is probably because of the shorter molecular chains of photo-degraded samples possessing higher mobility, which gather into bigger crystallites. However, further prolonging irradiation time leads to decrease of crystalline size because a large number of chemical defects (e.g., carbonyl groups) in the chains prevent further crystallization.

### Thermal properties

DSC thermograms of PP and PP/mLLDPE blends obtained during the first and second heating runs are shown in Figures 4–6. It is believed that the

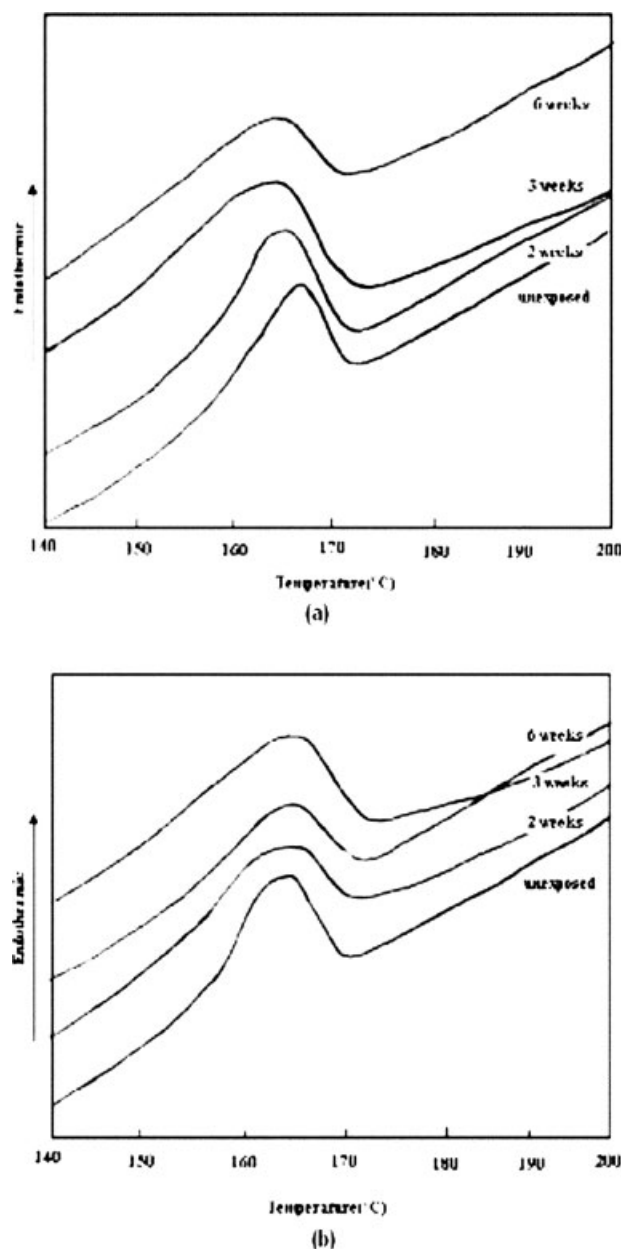


**Figure 6** DSC thermogram for PP/mLLDPE (80/20) after selected exposure time (a) first heating run, (b) second heating run.

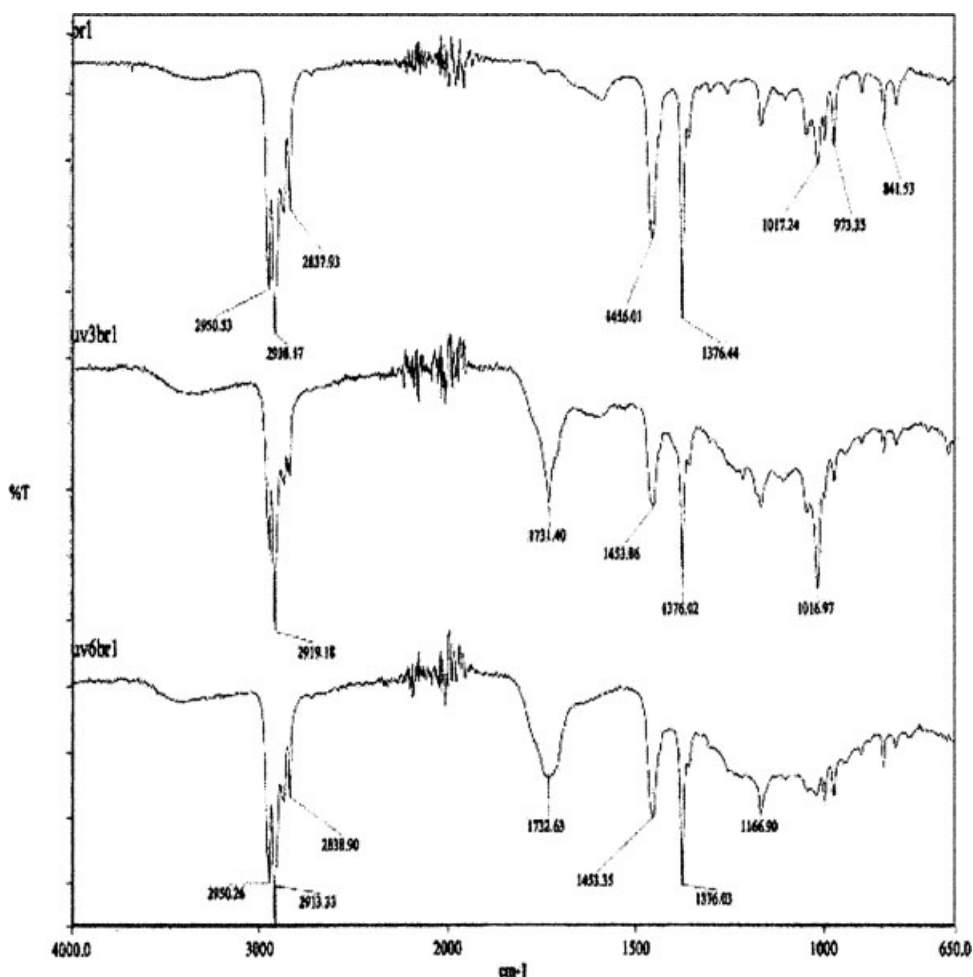


Figure 7 FTIR-ATR spectrum of PP unexposed and after exposure of 3 and 6 weeks.

second melting temperature reflects more precisely the effect of degraded molecules on the crystalline phase formation. The recrystallized material contains molecules that are both smaller (because of the chain scission processes) and defective (because of the presence of groups like carbonyls and hydro-peroxides); hence a reduction in the  $T_{m2}$  with exposure time has been observed.<sup>4</sup>

From various thermograms it is clear that the melting range is shifted to lower temperatures with increasing degradation. A comparison can be made with PP and PP/mLLDPE blend systems. It is observed that melting point of PP during the first and second heating run decreases significantly with exposure time. However, melting point of PP/mLLDPE (80/20) blend system remains unchanged throughout the exposure time.

The decrease in melting temperature of PP is probably because of the chain-scission, which causes reduction in molecular weight. It can thus be assumed that with the incorporation of mLLDPE in PP, disentanglement of the polymer matrix during photo-degradation would be much more difficult

because of the hindrance of hexyl branches, thus slowing down the chain-scission event.

#### FTIR-ATR

Figures 7–9 shows the FTIR-ATR spectra of PP and their blend systems with UV exposure of 3 and 6 weeks. The FTIR spectra of the unexposed samples showed traces of carbonyl groups, probably attributed to thermal oxidation during processing. The bands appearing at 1456 and 1376  $\text{cm}^{-1}$  in the unexposed sample are assigned to C–H bending vibration. Characteristic peaks of PP at 995 and 970  $\text{cm}^{-1}$  are also observed. The main products of degradation, carbonyls and hydro-peroxides, are easily observed, respectively in the wavelength ranges 1700–1800  $\text{cm}^{-1}$  and 3300–3600  $\text{cm}^{-1}$  as shown in the spectrum. These peaks tend to be fairly broad because they are the result of absorption by different products of degradation. In the UV exposed PP and PP/mLLDPE blend systems, the generation of carbonyl group at 1731, 1595  $\text{cm}^{-1}$  and the broad background peak at around 1000–1300  $\text{cm}^{-1}$  is observed.

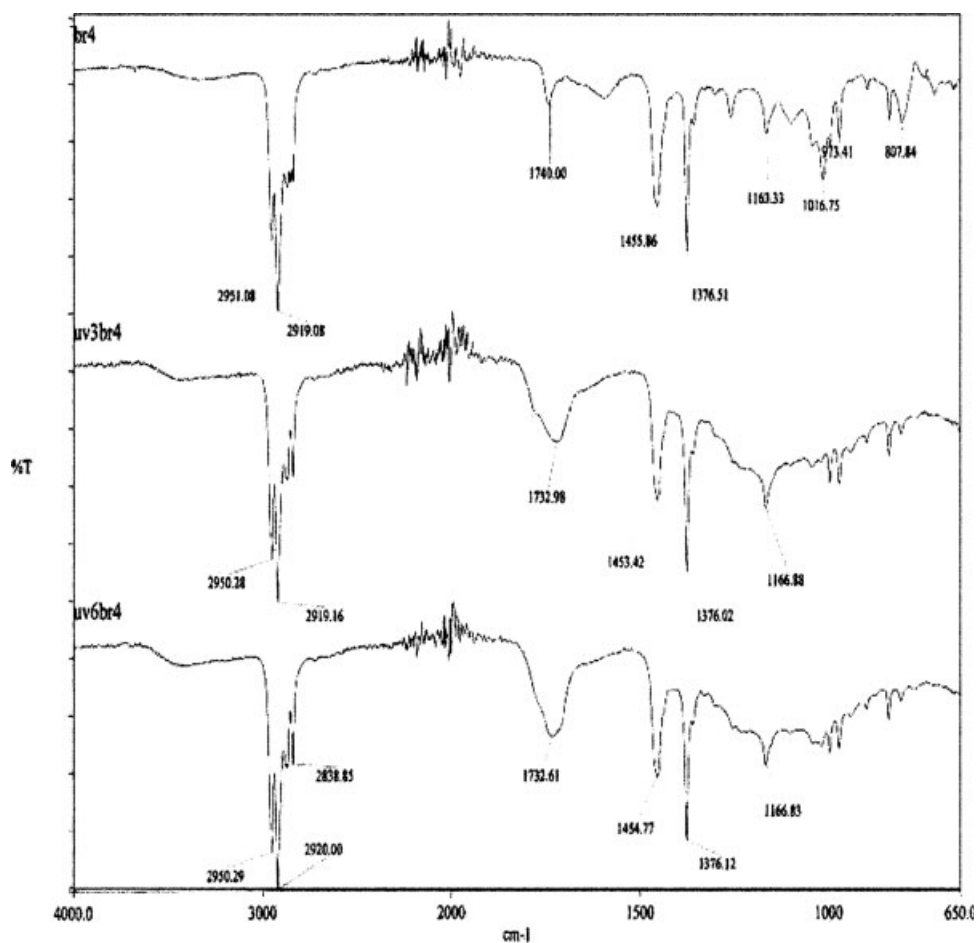


Figure 8 FTIR-ATR spectrum of PP/mLLDPE (90/10) unexposed and after exposure of 3 and 6 weeks.

This broad background peak was thought to appear as C—O stretching and O—H bending mode. It is observed that PP degraded significantly than PP/mLLDPE (80/20) blend systems.

The carbonyl indices obtained from the FTIR spectra are used to characterize the degree of oxidation of PP and PP/mLLDPE blend systems, as described in the experimental section. Figure 10 shows the changes in carbonyl region indices of PP and PP/mLLDPE blend systems with UV exposure time. The carbonyl index of PP and PP/mLLDPE blend systems increases apparently with UV exposure. However the carbonyl index of PP is higher than that of PP/mLLDPE (90/10), whereas PP/mLLDPE (80/20) displays the least carbonyl index, manifesting that PP/mLLDPE (80/20) is the most stable against UV exposure followed by PP/mLLDPE (90/10) and PP.

### Mechanical properties

Measurement of mechanical properties provides an excellent estimation of degradation from accelerated aging test. Hence UV radiation resistance of polymeric

material can be evaluated by measuring elongation at break and tensile modulus.

The tensile modulus ( $E$ ) of PP and PP/mLLDPE blend systems is found to increase during UV exposure. For PP, the tensile modulus increased significantly up to 3 weeks and after that it decreased. On the other hand, the tensile modulus of PP/mLLDPE (80/20) blend systems do not show much difference, as indicated in Figure 11(a).

The stiffness of semicrystalline polymer is primarily influenced by the degree of crystallinity ( $X$ ). The evolution of the tensile modulus should therefore, correlate with the variation of percent crystallinity ( $\%X$ ) as a function of UV exposure time. It is observed that percent crystallinity ( $\%X$ ) of PP increases with UV exposure time up to 3 weeks; further prolonging the exposure time, the crystallinity begin to decrease. The same trend is observed in tensile modulus. The increase in  $X$  and  $E$  is believed to be linked to degradation. The formation of new crystalline domains in UV degraded samples is often ascribed to chemi-crystallization.<sup>3</sup> This refers to the oxidation-induced cleavage of tie-molecules or entangled chains in the amorphous regions of the

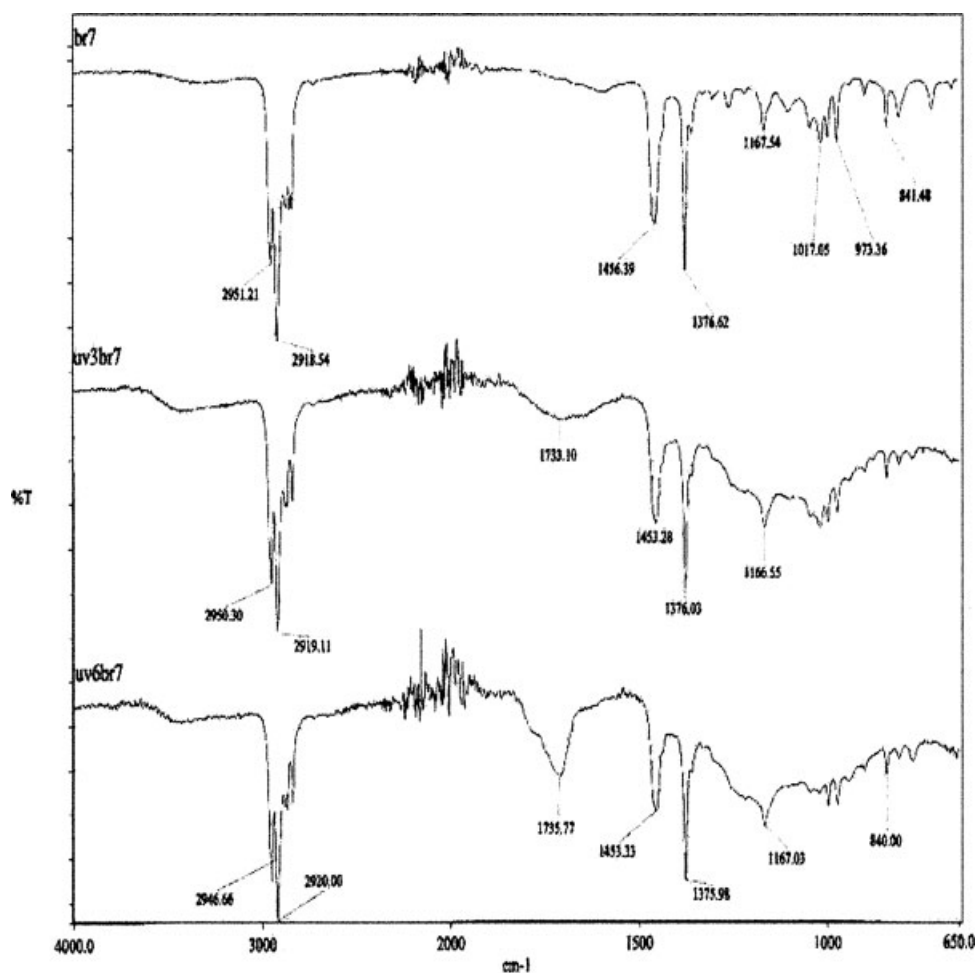


Figure 9 FTIR-ATR spectrum of PP/mLLDPE (80/20) unexposed and after exposure of 3 and 6 weeks.

polymer and the incorporation of the freed chain ends or segments into new crystalline domains at the lamellar surfaces or within the amorphous regions.<sup>2,3</sup>

PP and PP/mLLDPE blend systems displayed a highly ductile behavior in the unexposed state. The PP samples, however, underwent a ductile–brittle transition with UV exposure. Figure 11(b) shows the elongation at break ( $E_b$ ) for PP and PP/mLLDPE blend systems over a period of 6 weeks. PP experienced a decline in  $E_b$ , whereas there is not much reduction in  $E_b$  in the case of PP/mLLDPE (80/20) blends. It is very obvious that the decline in elongation at break of the samples, especially PP, is caused by extensive chain scission in the samples, causing the break down of tie chain molecules and entanglements, which are especially detrimental to the ductility of the polymer as it had been proved by several authors.<sup>4</sup> In case of PP/mLLDPE blends, it has to be kept in mind that diffusional hindrance may retard volatilization of the PP degradation products from the molten blend and give an apparent stabilization effect.

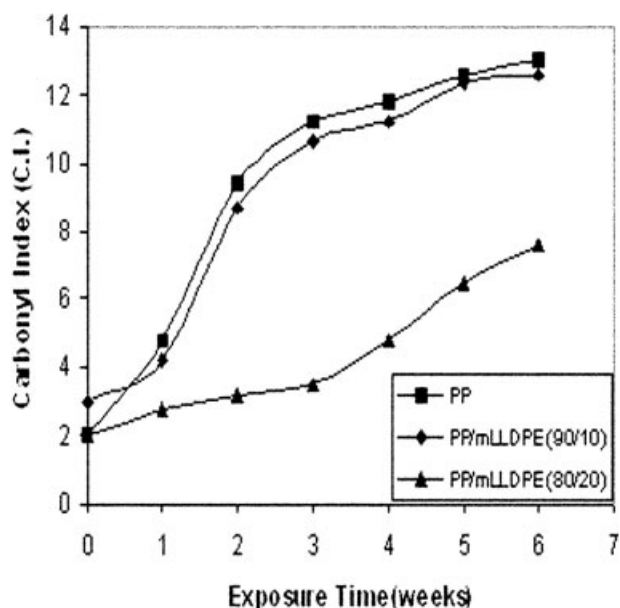
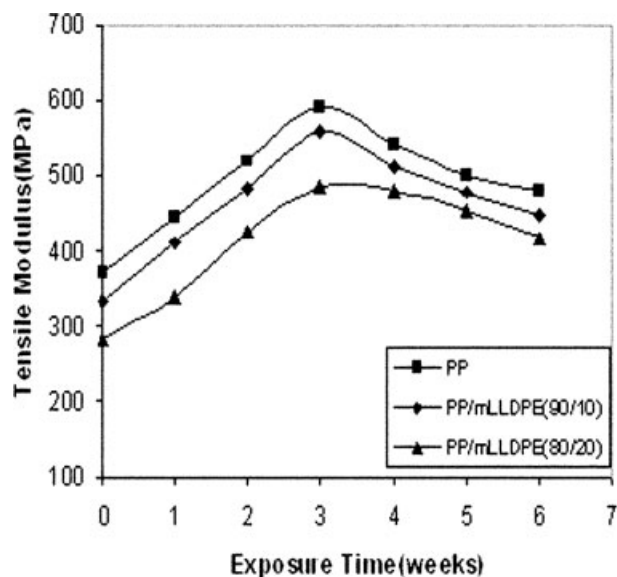
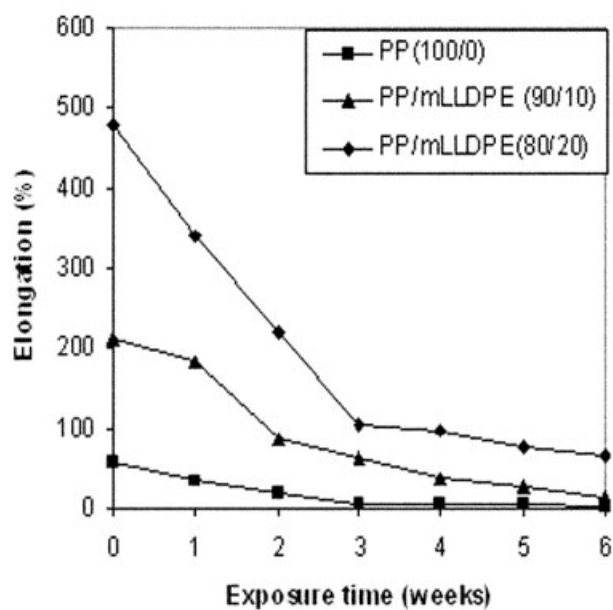


Figure 10 Carbonyl index of PP and PP/mLLDPE blend systems.





(a)



(b)

**Figure 11** Effect of exposure time on the (a) tensile modulus ( $E$ ) (b) elongation at break ( $E_b$ ) of PP and PP/mLLDPE blends.

### CONCLUSION

PP blends with mLLDPE in different compositional ratios prepared were exposed to QUV lamp chamber for photo-oxidative degradation. The following conclusions may be drawn:

1. Crystallization behavior of PP and PP/mLLDPE (80/20) blend systems was observed by XRD and DSC. The highest values of percent crystallinity (%X) are observed for the PP and the lowest ones for PP/mLLDPE (80/20) blend systems.
2. The results from the measurements of FTIR-ATR and mechanical properties have shown that PP/mLLDPE (80/20) has the highest UV stability, followed by PP/mLLDPE (90/10) and then PP.
3. The blending of PP and mLLDPE increases the oxidative stability of the PP because of the dilution of tertiary alkyl radicals of PP by the domains of mLLDPE.

### References

1. Zweifel, H. Stabilization of Polymeric Materials; Springer: Berlin, 1998.
2. Rabek, J. F. Polymer Photo Degradation—Mechanism and Experimental Methods; Chapman and Hall: London, 1995.
3. Rabello, M. S.; White, J. R. *Polymer* 1997, 38, 6379.
4. Rabello, M. S.; White, J. R. *Polym Degrad Stab* 1997, 56, 55.
5. Tang, L.; Wu, Q.; Qu, B. *J Appl Polym Sci* 2005, 95, 270.
6. Sadrmohaghegh, C.; Scott, G.; Setoudeh, E. *Polym Degrad Stab* 1981, 6, 469.
7. La Mantia, F. P. *Polym Degrad Stab* 1986, 14, 241.
8. Valenza, A.; La Mantia, F. P. *AJSE* 1988, 13, 497.
9. Al-Malika, S.; Amir, E. J. *Polym Degrad Stab* 1986, 16, 347.
10. Waldman, W. R.; DePaoli, A. M. *Polym Degrad Stab* 1998, 60, 301.
11. Abdel-Bary, E. M.; Abdel-Razik, E. A.; Abdelaal, M. Y.; El-Sherbiny, I. M. *Polym Plast Technol Eng* 2005, 44, 847.
12. Meligi, G.; Yoshii, F.; Sasaki, T.; Makuuchi, K.; Rabie, A. M.; Nishimoto, S. *Polym Degrad Stab* 1997, 57, 241.
13. Foster, G. N.; Wasserman, S. H.; Yacka, D. J. *Angew Makromol Chem* 1997, 252, 11.
14. Hamid, S. H. *J Appl Polym Sci* 2000, 78, 1591.
15. Hoang, M. E.; Allen, N. S.; Liauw, C. M.; Fontan, E.; Lafuente, P. *Polym Degrad Stab* 2006, 91, 1356.
16. Hoang, M. E.; Allen, N. S.; Liauw, C. M.; Fontan, E.; Lafuente, P. *Polym Degrad Stab* 2006, 91, 1363.
17. Al-Malika, S.; Peng, X.; Watson, H. *Polym Degrad Stab*, 2006, 91, 3131.
18. Gupta, A. P.; Saroop, U. K.; Gupta, V. *Polym Plast Technol Eng* 2007, 46, 281.
19. Gupta, A. P.; Saroop, U. K.; Gupta, V. *Polym Plast Technol Eng*, to appear.
20. ASTM D 4329-99; Standard Practice for Fluorescent UV Exposure of Plastics, ASTM: West Conshohocken, PA.
21. Turner-Jones, A.; Aizlewood, J. M.; Beckett, D. R. *Macromol Chem* 1964, 75, 134.
22. Quirk, R. P.; Alsamarraie, M. A. A. In: *Polymer Handbook*; Brandrup J., Immergut, E. H., Eds.; Wiley: New York, 1990; Vol. 27.
23. Kotek, J.; Kelnar, I.; Baldrian, J.; Raab, M. *Eur Polym J* 2004, 40, 2731.